VIP Electrochemistry Very Important Paper

International Edition: DOI: 10.1002/anie.201900109
German Edition: DOI: 10.1002/ange.201900109

# Superhydrophilic Phytic-Acid-Doped Conductive Hydrogels as Metal-Free and Binder-Free Electrocatalysts for Efficient Water Oxidation

*Qi Hu, Guomin Li, Xiufang Liu, Bin Zhu, Xiaoyan Chai, Qianling Zhang, Jianhong Liu, and Chuanxin He**

***Abstract:*** *Recently, metal-free, heteroatom-doped carbon nanomaterials have emerged as promising electrocatalysts for the oxygen evolution reaction (OER), but their synthesis is a tedious process involving energy-wasting calcination. Molecular electrocatalysts offer attractive catalysts for the OER. Here, phytic acid (PA) was selected to investigate the OER activity of carbons in organic molecules by DFT calculations and experiments. Positively charged carbons on PA were very active towards the OER. The PA molecules were fixed into a porous, conductive hydrogel with a superhydrophilic surface. This outperformed most metal-free electrocatalysts. Besides the active sites on PA, the high OER activity was also related to the porous and conductive networks on the hydrogel, which allowed fast charge and mass transport during the OER. Therefore, this work provides a metal-free, organic-molecule-based electrocatalyst to replace carbon nanomaterials for efficient OER.*

The electrochemical oxygen evolution reaction (OER) has gained ever increasing attention due to its essential role in various renewable technologies, such as water splitting and rechargeable metal-air batteries.[1] Unfortunately, the OER involves multi-electron transfer, often undergoes a substantial overpotential, and is of low efficiency.[2] As such, it is desirable to explore highly active electrocatalysts for boosting the OER. Though the state-of-the-art $RuO_2$ and $IrO_2$ electrocatalysts are very active towards the OER,[3] their high cost and scarcity make their widespread application unlikely. To this end, great efforts have been devoted to developing low-cost transition-metal (TM)-based materials (i.e. oxides, sulfides, phosphides, and hydroxides) for OER.[4] However, up to now, most of them still suffer from low conductivity and poor stability for OER. Besides that, to reduce the impact on environment, it is imperative to reduce metal usage or even develop efficient metal-free electrocatalysts. As such, metal-free, heteroatom (i.e. N, P, and S)-doped carbon materials (i.e. graphene and carbon nanotubes) have emerged as alternative electrocatalysts for the OER.[5] The heteroatom doping is believed to induce the charge redistribution of carbon atoms, thereby boosting their activity towards the OER.[6] Nevertheless, these doped carbon nanomaterials are often prepared through tedious multistep procedures, including energy-intensive pyrolysis and treatment with toxic chemicals. Therefore, it is highly attractive to search for other metal-free and readily available electrocatalysts for OER

Phytic acid (PA), also denoted as inositol hexaphosphoric acid, is a naturally abundant product in various plants, such as nuts, cereals, and legumes.[7] Because of the strong electronic affinity of phosphate groups, the carbons of the cyclohexane groups on PA should possess certain amount of positive charge. It is well reported that the N-doped carbon atoms with positive charges on nanomaterials are very active towards the OER due to their appropriate binding energy with intermediates of the OER.[6a,8] The positively charged carbons on PA may also have some activity towards the OER, which has not yet been investigated.

Conductive polymer-based hydrogels, with the intrinsic merits of high conductivity, excellent hydrophilicity, and strong structural stability,[9] are suitable substrates for electrochemical reactions involving gas, liquid, and solid, like the OER. Herein, a conductive and porous hydrogel composed of phytic-acid (PA)-doped polypyrrole (PPy; PA–PPy) was coated on a carbon cloth (PA–PPy/CC) via a modified dip–coat–dry method, representing an efficient and stable electrocatalyst for the OER in 1 M KOH. A combination of density functional theory (DFT) calculations and experimental results corroborated that the OER activity of PA–PPy/CC originated from the positively charged carbons on PA. Moreover, the porous and conductive PPy networks of PA–PPy/CC could markedly promote the charge and mass transfer during the OER, thereby facilitating the OER process. Impressively, the surface of the PA-doped hydrogel was superhydrophilic, which was advantageous for the contact between the electrocatalysts and the electrolyte to facilitate the electrolyte transport. To our knowledge, this is the first report exploring the possibility of utilizing PA-doped hydrogels as electrocatalysts for the OER, which could provide new directions for the synthesis and mechanism investigation of molecular electrocatalysts.

DFT calculations were performed on the PA molecules to study their activity towards the OER. At first, the structure of PA was optimized, in which three phosphate groups were staggered above the benzene ring and the other three below. (Supporting Information, Figure S1) Due to the strong

[*] Dr. Q. Hu, G. Li, X. Liu, B. Zhu, Dr. X. Chai, Prof. Q. Zhang, Prof. J. Liu, Prof. C. He
College of Chemistry and Environmental Engineering, Shenzhen University
Shenzhen, 518060 (China)
E-mail: Hecx@szu.edu.cn
Supporting information and the ORCID identification number(s) for the author(s) of this article can be found under: https://doi.org/10.1002/anie.201900109.

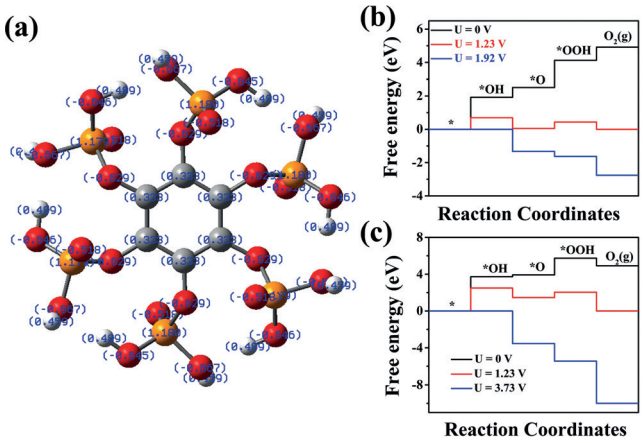


***Figure 1.*** a) Charge distribution of C (gray), P (orange), and O (red) elements on optimized structure of PA. Free energy diagram of b) C and c) P in PA for OER.

electron-withdrawing ability of phosphate groups, the carbons on PA possessed average charge of +0.333 e, based on the Mulliken charge analysis (Figure 1 a). Notably, the positively charged carbons (i.e. N-doped carbon) in nanomaterials are very active towards the OER.[8] As such, the activity of carbons in PA was examined by plotting the free energy diagram of carbons towards the OER under specified potentials. At a potential of 1.23 V, all steps of the OER were thermodynamically favorable on the carbons of PA, besides the first step of *OH adsorption (Figure 1 b), indicating that the adsorption of *OH was the rate-determining step of the OER. Upon increasing the potential to 1.92 V, the adsorption of *OH also became favorable. This meant that the overpotential of carbons in PA for the OER was 690 mV. However, in the case of phosphorus in PA, with an average charge of +1.180 e, the overpotential significantly increased to 2500 mV (Figure 1 c). This suggests that the phosphorus atoms in PA were not active for OER, even though they possessed positive charges. The optimized pathways of the OER on the carbons and phosphorus of PA are shown in Figures S2 and S3 in the Supporting Information. Based on the above calculations, with active sites of positively charged carbons, PA could be employed as an electrocatalyst for the OER.

As a proof-of-concept study, PA–PPy/CC was produced using a modified dip–coat–dry method. The crafting procedure is shown in Figure 2 a. Firstly, a piece of carbon cloth was immersed into a mixed solution of PA and pyrrole monomer (Py). Then a solution of ammonium persulfate ($(NH_4)_2S_2O_8$) was poured into the mixed solution. In this process, the $(NH_4)_2S_2O_8$ could trigger the polymerization of Py to generate the PA–PPy hydrogel, photographs of which can be seen in Figure S4 in the Supporting Information. Scanning electron microscopy (SEM) images of PA–PPy/CC show spherical particles of approximately 15 nm in diameter, interconnected to form networks on the fibers of the carbon cloth (Figure 2 b–d). Abundant macropores (ranging from 80 to 200 nm) could be observed in the networks (Figure 2 e). Furthermore, the pore size distribution, based on low-temperature-nitrogen adsorption–desorption shows that there were also mesopores

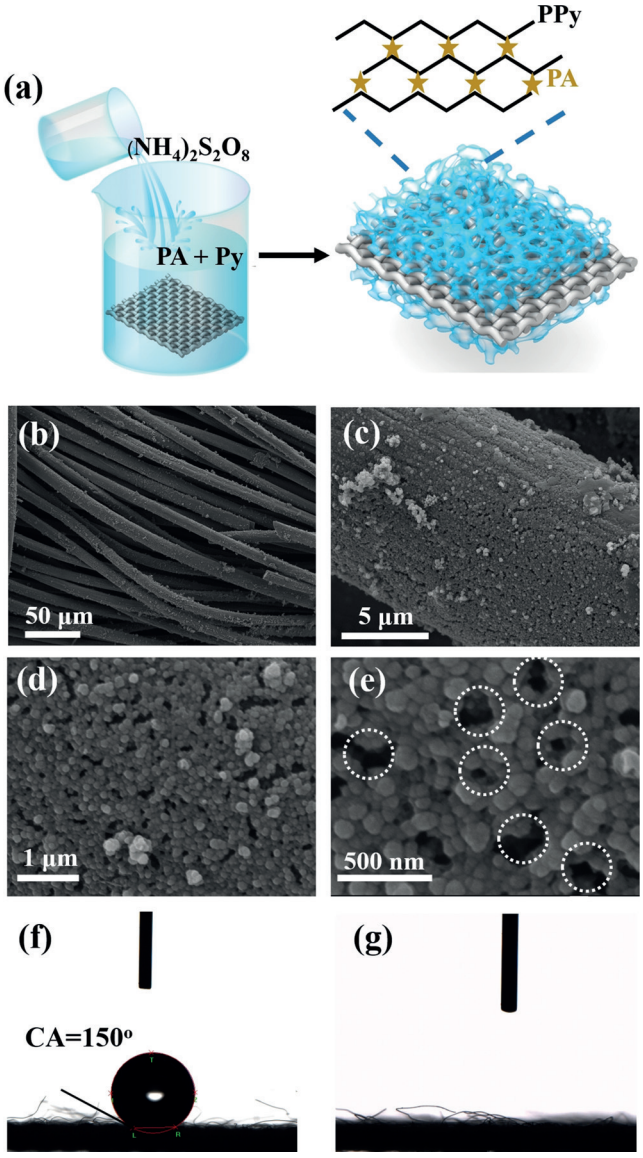


***Figure 2.*** a) Production process of phytic acid (PA)-doped polypyrrole (PPy; PA–PPy) hydrogel coated on carbon cloth (denoted PA–PPy/CC) via a modified dip–coat–dry method; b–d) SEM images of PA–PPy/CC with different magnifications; f and g) the contact angles of a drop of water on pure CC and PA–PPy/CC, respectively.

on the PA–PPy hydrogels (Supporting Information, Figure S5). Energy-dispersive X-ray spectroscopic (EDS) mapping provided further evidence that the C, N, and P elements were uniformly distributed on the porous network of PA–PPy/CC (Supporting Information, Figure S6). In the case of PPy/CC in absence of PA, the SEM images show compacted films coated on the carbon cloth without porous structures (Supporting Information, Figure S7). This implies that the PA could reduce the polymerization speed of Py to form porous, networked hydrogels. Notably, compared to pure CC (contact angle: 150°), the PA–PPy/CC possessed a superhydrophilic surface (contact angle: 0°; Figure 2 f, g). The superhydrophilic features of PA–PPy/CC are shown in the movie in the Supporting Information. The superhydrophilicity could be

  

due to the presence of abundant hydrophilic phosphate groups in PA and the porous nanostructures. Such a surface could markedly facilitate the contact between electrocatalysts and electrolyte, thereby favoring the transport of electrolyte.

X-ray photoelectron spectroscopy (XPS) was conducted to study the chemical composition of PA–PPy/CC. (Supporting Information, Figure S8) The survey XPS of PA–PPy/CC revealed the presence of C, N, P, and O elements. (Supporting Information, Figure S8a) The high-resolution spectra of C1s show one main peak at 284.6 eV, corresponding to the graphitic carbons on the carbon cloth, and one small shoulder peak at 288.1 eV, corresponding to the carbons in PA (Supporting Information, Figure S8b).[10] The relatively high binding energy of carbons in PA could be attributed to the electron transfer from carbons to phosphate groups in PA, in agreement with the above calculations. In the case of the N1s spectra, the strong peak at 399.9 eV could be attributed to the pyrrolic nitrogen in PPy (Supporting Information, Figure S8c).[11] The P2p spectra show a peak at 133.4 eV, corresponding to P–O in PA (Supporting Information, Figure S8d).[12] The Fourier transform infrared (FT-IR) spectra of PA–PPy/CC display a series of adsorption peaks at 1559.2, 1357.0, 1245 $cm^{-1}$, and 937 $cm^{-1}$ for PPy,[13] along with one strong peak at 1000.4 $cm^{-1}$ for PA[14] (Supporting Information, Figure S9), providing further evidence for the formation of PA–PPy hydrogels. Based on the SEM and XPS results, it is clear that the porous hydrogel containing PA and PPy can be coated on the carbon cloth through a facile dip–coat–dry method. With porous and conductive networks to transport electrons and electrolyte, the PA–PPy/CC is likely to possess high activity towards the OER.

The electrochemical performance of pure CC, PPy/CC (without PA), PA/CC (without PPy), and PA–PPy/CC towards the OER was studied in 1 M $O_2$-saturated KOH electrolyte. Clearly, the PA–PPy/CC possessed higher inherent activity with lower onset potential (1.51 V) and higher current density across the whole potential window, compared with other electrocatalysts. For example, at an overpotential of 570 mV, the PA–PPy/CC delivered a current density of 108.5 mA $cm^{-2}$, 8.7-, 6.0-, and 1.6-fold greater than that of CC, PPy/CC, and PA/CC, respectively. As both CC and PPy/CC (both without PA) displayed nearly negligible activity towards the OER, the observed OER activity of PA–PPy/CC can be derived from the PA. This is further confirmed by the high activity of PA/CC towards the OER. Notably, the PA–PPy/CC enabled a small overpotential of 340 mV to achieve a current density of 10 mA $cm^{-2}$ (Supporting Information, Figure S10), which compared favorably with most metal-free electrocatalysts[15] (Supporting Information, Table S2). Linear sweep voltammetry (LSV) of PA–PPy/CC was also recorded with different molar ratios of PPy/PA (Supporting Information, Figure S11) and determined that the optimum molar ratio of PPy/PA is 6. The reaction dynamics of the aforementioned eletrocatalysts towards the OER were then examined by extracting the slopes from Tafel curves. A small Tafel slope of 54.9 mV/dec can be seen for PA-PPy/CC, much smaller than that for CC (135.6 mV/dec), PPy/CC (140.5 mV/dec), and PA/CC (78.5 mV/dec), indicating a more beneficial OER process on PA–PPy/CC. This is in line

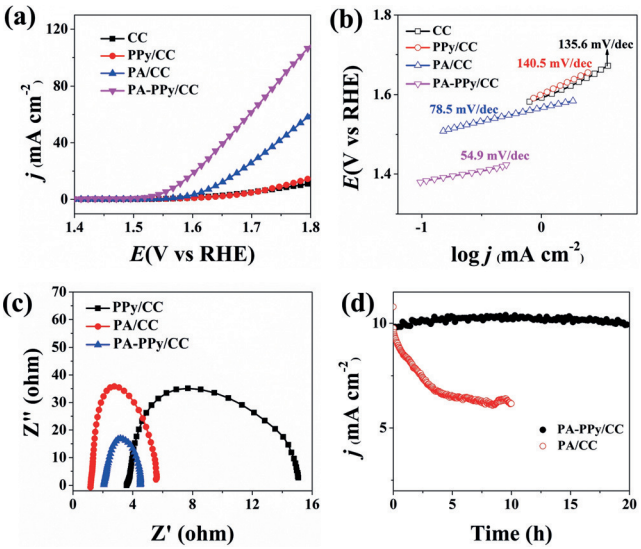


***Figure 3.*** a) Steady-state polarization profiles, and b) the corresponding Tafel plots of CC, PPy/CC, PA/CC, and PA–PPy/CC electrocatalysts for the OER in 1 M KOH. c) Electrochemical impedance spectroscopy (EIS) measurements on the aforementioned electrocatalysts. d) Current density vs. time (*I*–*t*) profiles of PA–PPy/CC and PA/CC for the OER at overpotentials of 340 and 410 mV, respectively.

with the OER activity displayed in the polarization curves (Figure 3a). To rule out the contribution of possible metal ions (i.e. $Fe^{3+}$) to the OER activity, $SCN^-$ ions were added into alkaline electrolyte to poison the metal ions. The finding that $SCN^-$ ions had no influence on the OER activity of PA–PPy/CC undoubtedly verifies that the OER activity for PA-PPy/CC was derived from the metal-free PA and not from metal impurities (Supporting Information, Figure S12).

The high activity of PA–PPy/CC may be also associated with conductive PPy networks enabling fast charge transfer during the OER. As such, electrochemical impedance spectroscopy (EIS) was performed on the three electrocatalysts (PPy/CC, PA/CC, and PA–PPy/CC) to test the resistance during the OER. As displayed in Figure 3c, compared with that of PPy/CC (4.5 Ω), the PA/CC had much a larger charge transfer resistance ($R_{ct}$; 11.5 Ω), signifying that the conductive PPy networks could markedly facilitate the charge transfer during the OER. Notably, the PA–PPy/CC displayed an even smaller $R_{ct}$ of 2.4 Ω, implying that the porous nanostructure is also important for the fast charge transfer. Interestingly, the PA/CC, PPy/CC, and PA–PPy/CC displayed different solution resistance, which may be attributed the pH change near the electrode surface, derived from the electrostatic interaction of positively charged carbon in PA and $OH^-$ in electrolyte. The long-term stability of OER electrocatalysts is a prerequisite for their practical usage. To this end, the stability of PA–PPy/CC was evaluated by chronoamperometry at an overpotential of 340 mV (Figure 3d). After 20 h of continuous OER, the current density of PA–PPy/CC remained almost unchanged, signifying the outstanding stability of PA–PPy/CC towards the OER. To further demonstrate the stability of PA–PPy/CC, SEM, XPS, and FT-IR measurements were conducted on PA–PPy/CC after

  

the stability test (Supporting Information, Figures S13–S15), which revealed that the PA–PPy/CC possessed outstanding structural stability. This also suggests that the OER activity of PA–PPy/CC originated from the PA molecules and not their decomposition products. In sharp contrast, the PA/CC suffered from a sharp current density loss of 40% over a 10 h stability test. This is ascribed to the loss of PA during OER, resulting from the good water solubility of PA. Therefore, in PA–PPy/CC, the PPy networks could act as stabilizers to prevent the loss of PA during long-term OER due to the strong hydrogen bonding interaction between PPy and PA.

The porous nanostructure of PA–PPy/CC may expose more active sites for OER. Therefore, the double layer capacitance ($C_{dl}$) of PPy/CC, PA/CC, and PA–PPy/CC was evaluated through cyclic voltammetry (CV) at different scan rates (Supporting Information, Figure S16). As expected, the $C_{dl}$ of PA–PPy/CC (1.85 mF cm$^{-2}$) was larger than that of PPy/CC (1.33 mF cm$^{-2}$) and PA/CC (0.61 mF cm$^{-2}$; Supporting Information, Figure S17). This shows that the porous nanostructure could enhance the surface area of PA–PPy/CC to expose more active sites for the OER. Therefore, the high activity of PA–PPy/CC is also related to the high surface area resulting from the porous nanostructure.

Based on above results, the excellent activity of PA–PPy/CC towards the OER can be attributed to the following aspects: 1) the PA molecules provided positively charged carbons with high activity towards the OER, as demonstrated by DFT calculations.; 2) the conductive PPy networks allowed fast charge transfer during the OER; 3) The porous nanostructure could not only expose more active sites for OER but also promote the charge and mass transport during the OER; 4) The PA–PPy hydrogel was directly grown on the carbon cloth without the usage of binders, which could eliminate the adverse effects of binders on the OER.

In summary, for the first time, we highlighted the excellent OER activity of positively charged carbons in organic molecules (i.e. phytic acid, denoted PA), as confirmed by both DFT calculations and experimental results. Moreover, we found that doping PA into conductive, porous hydrogels was a robust strategy for stabilizing PA, as well as enhancing the charge and mass transport of PA during the OER. The resulting PA-doped hydrogel possessed a superhydrophilic surface, which could significantly promote the contact between electrocatalysts and electrolyte, thereby promoting the electrolyte transport. Therefore, the porous, conductive hydrogels, comprising PA-doped polypyrrole (PPy; PA–PPy) supported on carbon cloth (PA–PPy/CC) displayed desirable activity towards the OER, such as a small overpotential of 340 mV at 10 mA cm$^{-2}$, a Tafel slope of 54.9 mV dec$^{-1}$, and a long-term stability of 20 h, surpassing most metal-free electrocatalysts.[16] Notably, the as-synthesized electrocatalysts are efficient, metal-free, binder-free, low-cost, environmentally friendly, and their production is easy to scale up. Therefore, this work opens up new doors to the development of low-cost and metal-free, organic-molecule-based electrocatalysts for the OER and other energy-related electrocatalysis applications.

## Acknowledgements

The financial support of the National Natural Science Foundation (NNSF) of China (21574084 and 21571131), the Natural Science Foundation of Guangdong (2017A040405066), and Shenzhen Government's Plan of Science and Technology (JCYJ20170817095041212 and JCYJ20170818091657056) are gratefully acknowledged.

## Conflict of interest

The authors declare no conflict of interest.

**Keywords:** hydrogel · metal-free electrocatalysts · oxygen evolution reaction · phytic acid · porous structures

**How to cite:** *Angew. Chem. Int. Ed.* **2019**, *58*, 4318–4322
*Angew. Chem.* **2019**, *131*, 4362–4366

[1] a) Q. Hu, X. Liu, B. Zhu, L. Fan, X. Chai, Q. Zhang, J. Liu, C. He, Z. Lin, *Nano Energy* **2018**, *50*, 212–219; b) Q. Wang, Y. Ji, Y. Lei, Y. Wang, Y. Wang, Y. Li, S. Wang, *ACS Energy Lett.* **2018**, *3*, 1183–1191; c) A. Indra, U. Paik, T. Song, *Angew. Chem. Int. Ed.* **2018**, *57*, 1241–1245; *Angew. Chem.* **2018**, *130*, 1255–1259.

[2] a) W.-J. Jiang, S. Niu, T. Tang, Q.-H. Zhang, X.-Z. Liu, Y. Zhang, Y.-Y. Chen, J.-H. Li, L. Gu, L.-J. Wan, J.-S. Hu, *Angew. Chem. Int. Ed.* **2017**, *56*, 6572–6577; *Angew. Chem.* **2017**, *129*, 6672–6677; b) Q. Gao, C.-Q. Huang, Y.-M. Ju, M.-R. Gao, J.-W. Liu, D. An, C.-H. Cui, Y.-R. Zheng, W.-X. Li, S.-H. Yu, *Angew. Chem. Int. Ed.* **2017**, *56*, 7769–7773; *Angew. Chem.* **2017**, *129*, 7877–7881; c) B. Zhu, Q. Hu, X. Liu, G. Li, L. Fan, Q. Zhang, J. Liu, C. He, *Chem. Commun.* **2018**, *54*, 10187–10190; d) Y. Zhao, X. Zhang, X. Jia, G. I. N. Waterhouse, R. Shi, X. Zhang, F. Zhan, Y. Tao, L.-Z. Wu, C.-H. Tung, D. O'Hare, T. Zhang, *Adv. Energy Mater.* **2018**, *8*, 1703585.

[3] L. C. Seitz, C. F. Dickens, K. Nishio, Y. Hikita, J. Montoya, A. Doyle, C. Kirk, A. Vojvodic, H. Y. Hwang, J. K. Norskov, T. F. Jaramillo, *Science* **2016**, *353*, 1011–1014.

[4] a) L. Xu, Q. Jiang, Z. Xiao, X. Li, J. Huo, S. Wang, L. Dai, *Angew. Chem. Int. Ed.* **2016**, *55*, 5277–5281; *Angew. Chem.* **2016**, *128*, 5363–5367; b) Q. Hu, X. Liu, B. Zhu, G. Li, L. Fan, X. Chai, Q. Zhang, J. Liu, C. He, *J. Power Sources* **2018**, *398*, 159–166; c) X. Xiao, C.-T. He, S. Zhao, J. Li, W. Lin, Z. Yuan, Q. Zhang, S. Wang, L. Dai, D. Yu, *Energy Environ. Sci.* **2017**, *10*, 893–899; d) C. Andronescu, S. Barwe, E. Ventosa, J. Masa, E. Vasile, B. Konkena, S. Möller, W. Schuhmann, *Angew. Chem. Int. Ed.* **2017**, *56*, 11258–11262; *Angew. Chem.* **2017**, *129*, 11411–11416.

[5] a) J. Zhang, Z. Zhao, Z. Xia, L. Dai, *Nat. Nanotechnol.* **2015**, *10*, 444; b) H. B. Yang, J. Miao, S.-F. Hung, J. Chen, H. B. Tao, X. Wang, L. Zhang, R. Chen, J. Gao, H. M. Chen, L. Dai, B. Liu, *Sci. Adv.* **2016**, *2*, e1501122; c) C. Hu, L. Dai, *Adv. Mater.* **2017**, *29*, 1604942.

[6] a) M. Li, L. Zhang, Q. Xu, J. Niu, Z. Xia, *J. Catal.* **2014**, *314*, 66–72; b) L. Li, H. Yang, J. Miao, L. Zhang, H.-Y. Wang, Z. Zeng, W. Huang, X. Dong, B. Liu, *ACS Energy Lett.* **2017**, *2*, 294–300; c) Z. Liu, Z. Zhao, Y. Wang, S. Dou, D. Yan, D. Liu, Z. Xia, S. Wang, *Adv. Mater.* **2017**, *29*, 1606207.

[7] a) A. J. Hatch, J. D. York, *Cell* **2010**, *143*, 1030-1030.e1; b) J. Song, B. Zhou, H. Zhou, L. Wu, Q. Meng, Z. Liu, B. Han, *Angew. Chem. Int. Ed.* **2015**, *54*, 9399–9403; *Angew. Chem.* **2015**, *127*, 9531–9535.

[8] a) T. Y. Ma, S. Dai, M. Jaroniec, S. Z. Qiao, *Angew. Chem. Int. Ed.* **2014**, *53*, 7281–7285; *Angew. Chem.* **2014**, *126*, 7409–7413; b) J.-C. Li, P.-X. Hou, S.-Y. Zhao, C. Liu, D.-M. Tang, M. Cheng,

  

F. Zhang, H.-M. Cheng, *Energy Environ. Sci.* **2016**, *9*, 3079 – 3084.
[9] a) L. Pan, G. Yu, D. Zhai, H. R. Lee, W. Zhao, N. Liu, H. Wang, B. C.-K. Tee, Y. Shi, Y. Cui, Z. Bao, *Proc. Natl. Acad. Sci. USA* **2012**, *109*, 9287 – 9292; b) Y. Shi, L. Pan, B. Liu, Y. Wang, Y. Cui, Z. Bao, G. Yu, *J. Mater. Chem. A* **2014**, *2*, 6086 – 6091; c) Z. Chen, J. W. F. To, C. Wang, Z. Lu, N. Liu, A. Chortos, L. Pan, F. Wei, Y. Cui, Z. Bao, *Adv. Energy Mater.* **2014**, *4*, 1400207.
[10] Y. Chang, F. Hong, C. He, Q. Zhang, J. Liu, *Adv. Mater.* **2013**, *25*, 4794 – 4799.
[11] Y. Song, W. Chen, C. Zhao, S. Li, W. Wei, Y. Sun, *Angew. Chem. Int. Ed.* **2017**, *56*, 10840 – 10844; *Angew. Chem.* **2017**, *129*, 10980 – 10984.
[12] Q. Hu, X. Liu, C. Tang, L. Fan, X. Chai, Q. Zhang, J. Liu, C. He, *Sustainable Energy Fuels* **2018**, *2*, 1085 – 1092.
[13] W. Sun, Z. Mo, *Polym. Bull.* **2014**, *71*, 2173 – 2184.
[14] Y. Li, Y. Song, J. Li, Y. Li, N. Li, S. Niu, *Ultrason. Sonochem.* **2018**, *42*, 18 – 25.
[15] J. Lai, S. Li, F. Wu, M. Saqib, R. Luque, G. Xu, *Energy Environ. Sci.* **2016**, *9*, 1210 – 1214.
[16] C. Mo, J. Jian, J. Li, Z. Fang, Z. Zhao, Z. Yuan, M. Yang, Y. Zhang, L. Dai, D. Yu, *Energy Environ. Sci.* **2018**, *11*, 3334 – 3341.

Manuscript received: January 3, 2019
Accepted manuscript online: February 2, 2019
Version of record online: February 20, 2019

  